Dynamic Energy Management for Smart-Grid-Powered Coordinated Multipoint Systems

Xin Wang, *Senior Member, IEEE*, Yu Zhang, *Student Member, IEEE*, Tianyi Chen, *Student Member, IEEE*, and Georgios B. Giannakis, *Fellow, IEEE*

Abstract—Due to increasing threats of global warming and climate change concerns, green wireless communications have recently drawn intense attention toward reducing carbon emissions. Aligned with this goal, the present paper deals with dynamic energy management for smart-grid powered coordinated multipoint (CoMP) transmissions. To address the intrinsic variability of renewable energy sources, a novel energy transaction mechanism is introduced for grid-connected base stations that are also equipped with an energy storage unit. Aiming to minimize the expected energy transaction cost while guaranteeing the worst-case users' quality of service, an infinite-horizon optimization problem is formulated to obtain the optimal downlink transmit beamformers that are robust to channel uncertainties. Capitalizing on the virtual-queue-based relaxation technique and the stochastic dual-subgradient method, an efficient online algorithm is developed yielding a feasible and asymptotically optimal solution. Numerical tests with synthetic and real data corroborate the analytical performance claims and highlight the merits of the novel approach.

Index Terms—CoMP systems, downlink beamforming, smart grids, high-penetration renewables, stochastic optimization, Lyapunov optimization.

I. INTRODUCTION

IN future 5G wireless standards, current cellular systems are envisioned to evolve into the so-termed heterogeneous networks (HetNets), which consist of distributed macro/micro/pico base stations (BSs) to cover overlapping areas of different sizes.L To deal with the severe inter-cell interference introduced by close proximity of many such HetNet BSs, coordinated multi-point (CoMP) processing has been proposed as a promising technique for efficient interference management [1]. In CoMP systems, BSs team up (possibly adaptively) to form clusters, where per-cluster BSs perform coordinated beamforming to serve the cell end users [2]–[4].

The increasing demand for energy-efficient transmissions is one of the main driving factors for CoMP systems. Due to the growing number of BSs in HetNets, the electricity bill becomes a major part of the operational expenditure of a cellular operator. Meanwhile, cellular networks contribute a considerable portion of the global *carbon footprint* [7]. The economic and ecological concerns advocate a *green communication* solution, where cellular BSs are powered by the electricity grid [2]–[4], [7]–[9]. However, the current grid infrastructure is on the verge of a major paradigm shift, migrating from the aging grid to a "smart" one. The smart grid has many new features and advanced capabilities including e.g., high penetration of distributed renewable energy sources (RES), and dynamic pricing based demand-side management (DSM) [10]–[13]. Full benefits of the RES (e.g., wind and solar energy) can only be harnessed by properly mitigating its intrinsically stochastic nature, which however is a very challenging task. For instance, Fig. 1 exhibits the real data of hourly wind and solar power generation that depend on various meteorological factors including e.g., wind speed and direction, air density and pressure, sunlight, as well as temperature. In addition, annual, seasonal, diurnal and hourly patterns may change dramatically across regions.

A few recent works have considered the smart-grid powered CoMP transmissions [14]–[17]. A simplified smart grid level game was formulated in [14] for dynamic pricing; while [15] and [16] assumed that the energy harvested from RES is accurately available *a priori* through e.g., forecasting, which cannot be performed at the BSs. For a single BS supported by a combination of a renewable source and a storage unit, an adaptive energy management problem was cast as a stochastic program, and was further approximated with finite discrete scenarios, in [17]. The case of multiple BSs with transmit beamforming designs has not been considered therein. Building on realistic models, our recent work [18] addressed robust energy management and transmit-beamforming designs that minimize the worst-case energy transaction cost subject to the worst-case user quality-of-service (QoS) guarantees for the CoMP downlink with RES and DSM. Leveraging novel
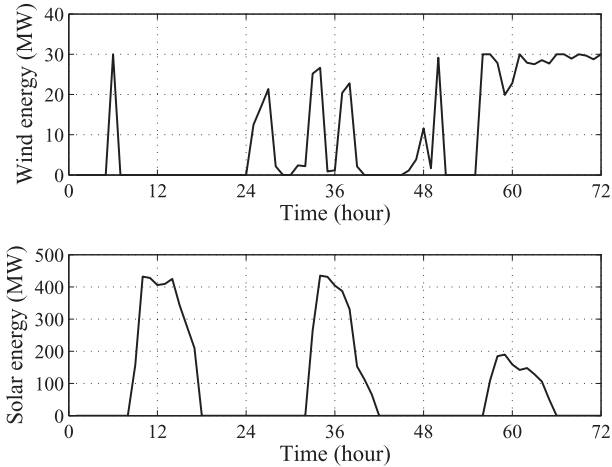
Fig. 1. Hourly wind power generation of a farm near the city of Boulder, Colorado during Jan. 01–03, 2006 [5]; and solar PV generation of the California ISO during Feb. 26–28, 2015 [6].

optimization tools, the resultant problem became a convex program. A Lagrange dual based subgradient solver was then proposed to find the optimal energy-management strategy and transmit-beamforming vectors.

Assuming that the generated random RES lies in a certain known region, [18] dealt with *offline*, robust, ahead-of-time resource management over a given finite horizon. However, the computational complexity of the algorithm proposed by [18] becomes prohibitively high as the scheduling time horizon grows large. In the present paper, we pursue an *online* control approach, which dynamically makes *instantaneous* decisions without prior knowledge of the probability density function (pdf) of the underlying (generally correlated) random processes. The resource allocation task is formulated as an infinite time horizon problem with the goal of minimizing the time-average energy transaction cost. To obtain low-complexity operating points, we first adopt a virtual-queue based relaxation technique [19], [20], to decouple the decision variables across time. The resulting transaction cost minimization problem is then convexified using semidefinite relaxation to facilitate the development of an efficient stochastic solver. Leveraging the stochastic dual-subgradient method, we develop a virtual-queue based online control algorithm. Relying on the so-called Lyapunov optimization technique [21], and the revealed characteristics of the optimal schedules, we formally establish that the proposed algorithm yields a feasible and asymptotically optimal resource management strategy for the original problem.

The rest of the paper is organized as follows. The system models are described in Section II. The proposed dynamic resource management scheme is developed in Section III. Analysis of the guaranteed performance is the subject of Section IV. Numerical tests are presented in Section V, followed by concluding remarks in Section VI.

Notation. Boldface lower (upper) case letters represent vectors (matrices); $\mathbb{C}^{N \times M}$, $\mathbb{R}^{N \times M}$, and $\mathbb{C}^N$ stand for spaces of $N \times M$ complex, real matrices, and $N \times 1$ complex vectors, respectively. $[a]^+ := \max\{a, 0\}$, and $\|\mathbf{a}\|$ denotes the ℓ_2-norm of $\mathbf{a}$. $(\cdot)'$ denotes transpose, and $(\cdot)^H$ conjugate transpose; $\mathrm{tr}(\mathbf{A})$ and

rank$(\mathbf{A})$ the trace and rank operators for matrix $\mathbf{A}$, respectively; $\mathrm{diag}(a_1, \ldots, a_M)$ denotes a diagonal matrix with diagonal elements $a_1, \ldots, a_M$; $|\cdot|$ the magnitude of a complex scalar; $\mathbf{A} \succeq \mathbf{0}$ signifies that $\mathbf{A}$ is positive semi-definite; and $\mathbb{E}$ denotes the expectation.

II. SYSTEM MODELS

With reference to Fig. 2, consider a cluster-based CoMP downlink system, where a set of $\mathcal{I} := \{1, \ldots, I\}$ BSs (e.g., macro/micro/pico BSs) serves a set of $\mathcal{K} := \{1, \ldots, K\}$ mobile end users. Each BS is equipped with M transmit antennas, while each user has a single receive antenna. Assume that BSs can harvest RES using wind turbines and solar panels, to support their transmission services. Furthermore, each BS can also buy energy from or sell energy to the main grid at dynamically changing market prices via a two-way energy trading mechanism. As energy consumption of future communication systems becomes a major concern, uninterrupted power supply type storage units can be installed at BSs not only to prevent power outage, but also provide opportunities to optimize the BS electricity bills. Specifically, in order to take advantage of energy price fluctuations, storage-enabled BSs do not have to consume or sell all their harvested energy on the spot, but can save it for later use.

Per CoMP cluster, all BSs are connected to a central controller through a low-latency backhaul network [3]. This controller collects not only the communication data from each BS, but also the energy trading prices via locally installed smart meters, and the grid-deployed communication/control links.

Suppose the slot-based transmissions experience quasi-static downlink channels, which are allowed to vary across slots but remain invariant within each slot. This is a legitimate assumption when the slot length is selected smaller than the channel coherence time. For convenience, the slot duration is also normalized to unity, so the terms "energy" and "power" will thus be interchangeably used throughout the paper.

A. CoMP Transmissions

Consider a scheduling horizon indexed by the set $\mathcal{T} := \{0, \ldots, T - 1\}$. Per slot t, let $\mathbf{h}_{ik}^t \in \mathbb{C}^M$ denote the vector channel from BS i to user k, for all $i \in \mathcal{I}$ and $k \in \mathcal{K}$. Let $\mathbf{h}_k^t := [\mathbf{h}_{1k}^t{}', \ldots, \mathbf{h}_{Ik}^t{}']'$ collect the channels from all BSs to user k. With linear transmit beamformers across all BSs, the vector signal transmitted to user k is $\mathbf{q}_k^t = \mathbf{w}_k^t s_k^t$, for all $k \in \mathcal{K}$, where s_k^t denotes the information-bearing symbol with unit energy, and $\mathbf{w}_k^t \in \mathbb{C}^{MI}$ represents the beamforming vector across the BSs linked with user k. Thus, the received signal at user k in slot t is

$$y_k^t = \mathbf{h}_k^t{}^H \mathbf{q}_k^t + \sum_{l \neq k} \mathbf{h}_k^t{}^H \mathbf{q}_l^t + n_k^t \qquad (1)$$

where $\mathbf{h}_k^t{}^H \mathbf{q}_k^t$ is the desired signal of user k; $\sum_{l \neq k} \mathbf{h}_k^t{}^H \mathbf{q}_l^t$ captures the inter-user interference in the same cluster; and n_k^t models the additive noise, as well as the possible downlink interference from other BSs outside this cluster. For simplicity,
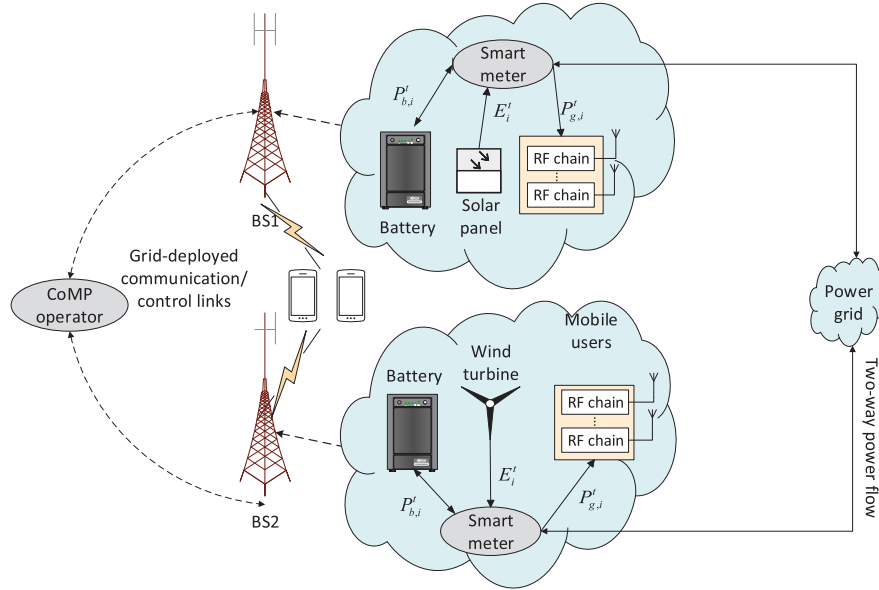
Fig. 2. A smart grid powered CoMP system. Two BSs with local renewable energy harvesting and storage devices implement two-way energy trading with the main grid.

n_k^t is assumed to be a circularly symmetric complex Gaussian (CSCG) random variable with zero mean and variance σ_k^2.

The signal-to-interference-plus-noise-ratio (SINR) of user k can be written as

$$\text{SINR}_k(\{\mathbf{w}_k^t\}) = \frac{|\mathbf{h}_k^{t\,H}\mathbf{w}_k^t|^2}{\sum_{l \neq k}(|\mathbf{h}_k^{t\,H}\mathbf{w}_l^t|^2) + \sigma_k^2} . \qquad (2)$$

The transmit power of BS i is given by

$$P_{x,i}^t = \sum_{k \in \mathcal{K}} \mathbf{w}_k^{t\,H}\mathbf{B}_i\mathbf{w}_k^t \qquad (3)$$

where the $MI \times MI$ matrix

$$\mathbf{B}_i := \text{diag}\left(\underbrace{0,\ldots,0}_{(i-1)M}, \underbrace{1,\ldots,1}_{M}, \underbrace{0,\ldots,0}_{(I-i)M}\right)$$

selects the corresponding rows out of $\{\mathbf{w}_k^t\}_{k \in \mathcal{K}}$ to form the i-th BS's transmit-beamforming vector.

The channel state information $\mathbf{h}_k^t$ is always imperfectly known *a priori* in practice. Relying on past channel measurements and/or reliable channel predictions, we postulate an additive error model $\mathbf{h}_k^t = \hat{\mathbf{h}}_k^t + \boldsymbol{\delta}_k^t$, where $\hat{\mathbf{h}}_k^t$ is the estimated channel known at the BSs. The uncertainty of this estimate is bounded by a spherical region [22]

$$\mathcal{H}_k^t := \left\{ \hat{\mathbf{h}}_k^t + \boldsymbol{\delta}_k^t \mid \|\boldsymbol{\delta}_k^t\| \leq \epsilon_k^t \right\}, \quad \forall k, t \qquad (4)$$

where $\epsilon_k^t > 0$ specifies the radius of $\mathcal{H}_k^t$. The worst-case SINR of user k can be expressed as [cf. (2)]

$$\widetilde{\text{SINR}}_k(\{\mathbf{w}_k^t\}) := \min_{\mathbf{h}_k^t \in \mathcal{H}_k^t} \frac{|\mathbf{h}_k^{t\,H}\mathbf{w}_k^t|^2}{\sum_{l \neq k}(|\mathbf{h}_k^{t\,H}\mathbf{w}_l^t|^2) + \sigma_k^2} . \qquad (5)$$

With γ_k denoting user k's target SINR, QoS per end user can be guaranteed by the constraint

$$\widetilde{\text{SINR}}_k(\{\mathbf{w}_k^t\}) \geq \gamma_k, \quad \forall k. \qquad (6)$$

B. Smart Grid Operations

Featuring smart grid operations, each BS can exploit RES with harvesting facilities, and store the energy for future use using onsite storage units. Let $\mathbf{e}^t := [E_1^t, \ldots, E_I^t]'$ collect the harvested renewables in slot t across all BSs. For simplicity, we assume that $\mathbf{e}^t$ evolves as an independent and identically distributed (i.i.d.) random process.

Let C_i^0 denote the initial amount of stored energy, and C_i^t the state of charge (SoC) of BS i at the beginning of slot t. Each storage unit (e.g., battery) has a finite capacity $C_i^{\max}$. A minimum level $C_i^{\min}$ is also required at any time for the sake of the battery health.[1] With $P_{b,i}^t$ denoting the battery charging ($P_{b,i}^t > 0$) or discharging ($P_{b,i}^t < 0$) amount at slot t, the battery dynamics are described by the recursion

$$C_i^{t+1} = C_i^t + P_{b,i}^t, \quad \forall i, t \qquad (7)$$

Due to physical constraints, the amount of power (dis-)charged is bounded by

$$P_{b,i}^{\min} \leq P_{b,i}^t \leq P_{b,i}^{\max} \qquad (8)$$

where $P_{b,i}^{\min} < 0$, and $P_{b,i}^{\max} > 0$.

Per BS i, the total energy consumption $P_{g,i}^t$ consists of the beamformers' transmitting power $P_{x,i}^t$, and a constant power

---

[1] Batteries become unreliable with high depth-of-discharge (DoD), which is the percentage of maximum charge removed during a discharge cycle. High DoD can be avoided by maintaining a minimum level $C_i^{\min}$. Such a level could be also required to support the BS operation in the event of a grid outage. Hence, we have $C_i^{\min} \leq C_i^t \leq C_i^{\max}$, for all $i \in \mathcal{I}$ and $t \in \mathcal{T}$.

$P_{c,i} > 0$ consumed by other components such as air conditioning, data processor, and circuits [9], [16]. Therefore, it holds that

$$P_{g,i}^t = P_{c,i} + P_{x,i}^t/\xi = P_{c,i} + \sum_{k \in \mathcal{K}} \mathbf{w}_k^{t\,H} \mathbf{B}_i \mathbf{w}_k^t/\xi$$

where $\xi > 0$ denotes the power amplifier efficiency, which can be set to $\xi = 1$ without loss of generality. The total consumption $P_{g,i}^t$ is bounded by $P_{g,i}^{\max}$.

The main grid can supply the needed $P_{g,i}^t$ if the harvested renewables are insufficient. In order to reduce operational costs, each BS can also sell its surplus energy (whenever the renewables are abundant) back to the grid via the two-way trading mechanism. To this end, it is clear that the shortage energy for BS i that needs to be purchased from the grid is $[P_{g,i}^t - E_i^t + P_{b,i}^t]^+$, while the surplus energy is $[E_i^t - P_{g,i}^t - P_{b,i}^t]^+$.

With α^t and β^t denoting the buying and selling prices, respectively, the condition $\alpha^t \geq \beta^t$ is imposed to avoid meaningless buy-and-sell activities. Per slot t, the transaction cost of BS i is therefore given by

$$G(P_{g,i}^t, P_{b,i}^t) := \alpha^t [P_{g,i}^t - E_i^t + P_{b,i}^t]^+ \\ - \beta^t [E_i^t - P_{g,i}^t - P_{b,i}^t]^+. \quad (9)$$

Note that at any time slot each BS can either buy electricity at price α^t, or sell surplus to the grid at the price β^t.

To simplify performance analysis, suppose that the prices $\{\alpha^t, \beta^t\}$ are i.i.d. across time. However, both the harvested renewable energy $\{e^t\}$ and the prices $\{\alpha^t, \beta^t\}$ can be non-i.i.d., and even negatively correlated with each other in practice [23]. For such a case, it is worth stressing that our proposed algorithm in the sequel can be applied without any modification. Yet, performance guarantees in the non-i.i.d. case must be obtained by utilizing the more sophisticated delayed Lyapunov drift techniques along the lines of e.g. [21].

III. DYNAMIC MANAGEMENT ALGORITHM

Based on the models of Section I, we consider the optimal energy management for transmit beamforming in a CoMP cluster. Over the scheduling horizon $\mathcal{T}$, the central controller of the CoMP cluster seeks an optimal schedule for cooperative transmit beamforming vectors $\{\mathbf{w}_k^t\}_{k,t}$ and battery charging energy $\{P_{b,i}^t\}_{i,t}$, in order to minimize the total network cost $\sum_{t \in \mathcal{T}} \sum_{i \in \mathcal{I}} G(P_{g,i}^t, P_{b,i}^t)$, while satisfying the user QoS guarantees $\widetilde{\mathrm{SINR}}_k(\{\mathbf{w}_k^t\}) \geq \gamma_k, \forall k, t$. For notational brevity, we introduce the auxiliary variables $P_i^t := P_{g,i}^t + P_{b,i}^t$, and formulate the problem of interest as

$$\underset{\{\mathbf{w}_k^t, P_{b,i}^t, C_i^t, P_i^t\}}{\text{minimize}} \lim_{T \to \infty} \frac{1}{T} \sum_{t=0}^{T-1} \sum_{i \in \mathcal{I}} G(P_i^t) \quad (10a)$$

s. t.

$$P_i^t = P_{c,i} + \sum_{k \in \mathcal{K}} \mathbf{w}_k^{t\,H} \mathbf{B}_i \mathbf{w}_k^t + P_{b,i}^t, \quad \forall i, t \quad (10b)$$

$$0 \leq P_{c,i} + \sum_{k \in \mathcal{K}} \mathbf{w}_k^{t\,H} \mathbf{B}_i \mathbf{w}_k^t \leq P_{g,i}^{\max}, \quad \forall i, t \quad (10c)$$

$$C_i^{t+1} = C_i^t + P_{b,i}^t, \quad \forall i, t \quad (10d)$$

$$C_i^{\min} \leq C_i^t \leq C_i^{\max}, \quad \forall i, t \quad (10e)$$

$$P_{b,i}^{\min} \leq P_{b,i}^t \leq P_{b,i}^{\max}, \quad \forall i, t \quad (10f)$$

$$\widetilde{\mathrm{SINR}}_k(\{\mathbf{w}_k^t\}) \geq \gamma_k, \quad \forall k, t. \quad (10g)$$

A. Reformulation and Relaxation

With $\psi^t := (\alpha^t - \beta^t)/2$ and $\phi^t := (\alpha^t + \beta^t)/2$, it follows readily from (9) that:

$$G(P_i^t) = \psi^t |P_i^t - E_i^t| + \phi^t (P_i^t - E_i^t).$$

Since $\alpha^t > \beta^t > 0$, we have $\phi^t > \psi^t > 0$. It is then clear that $G(P_i^t)$ is a convex function of P_i^t.

Except for (10b), (10c), and (10g), all other constraints are convex per slot t. We next rely on the popular semidefinite program (SDP) relaxation technique to convexify these constraints. Using the definitions of $\mathcal{H}_k^t$ and $\widetilde{\mathrm{SINR}}_k(\{\mathbf{w}_k^t\})$, the constraint (10g) can be rewritten as

$$F_k(\boldsymbol{\delta}_k^t) \geq 0 \text{ for all } \boldsymbol{\delta}_k^t \text{ such that } \boldsymbol{\delta}_k^{t\,H} \boldsymbol{\delta}_k^t \leq (\epsilon_k^t)^2 \quad (11)$$

where

$$F_k(\boldsymbol{\delta}_k^t)$$
$$:= \left(\hat{\mathbf{h}}_k^t + \boldsymbol{\delta}_k^t\right)^H \left(\frac{\mathbf{w}_k^t \mathbf{w}_k^{t\,H}}{\gamma_k^t} - \sum_{l \neq k} \mathbf{w}_l^t \mathbf{w}_l^{t\,H}\right) \left(\hat{\mathbf{h}}_k^t + \boldsymbol{\delta}_k^t\right) - \sigma_k^2.$$

Using (11) and upon applying the well-known S-procedure in robust optimization [24], the original problem (10) can be reformulated as an SDP with rank constraints.

Specifically, with $\mathbf{X}_k^t := \mathbf{w}_k^t \mathbf{w}_k^{t\,H} \in \mathbb{C}^{MI \times MI}$, it clearly holds that $\mathbf{X}_k^t \succeq \mathbf{0}$ and $\mathrm{rank}(\mathbf{X}_k^t) = 1$. Using the S-procedure, (11) can be transformed as

$$\boldsymbol{\Gamma}_k^t := \begin{pmatrix} \mathbf{Y}_k^t + \tau_k^t \mathbf{I} & \mathbf{Y}_k^t \tilde{\mathbf{h}}_k^t \\ \tilde{\mathbf{h}}_k^{t\,H} \mathbf{Y}_k^{t\,H} & \tilde{\mathbf{h}}_k^{t\,H} \mathbf{Y}_k^t \tilde{\mathbf{h}}_k^t - \sigma_k^2 - \tau_k^t(\epsilon_k^t)^2 \end{pmatrix} \succeq \mathbf{0} \quad (12)$$

where $\tau_k^t \geq 0$ and $\mathbf{Y}_k^t := \frac{1}{\gamma_k} \mathbf{X}_k^t - \sum_{l \neq k} \mathbf{X}_l^t$.

Introduce auxiliary variables τ_k^t and drop the rank constraints $\mathrm{rank}(\mathbf{X}_k^t) = 1, \forall k, t$; further, remove the variables $\{P_{b,i}^t\}$ by combining constraints (10b) with (10d). We can then transform (10) to

$$G^* := \underset{\{\mathbf{X}_k^t, \tau_k^t, P_i^t, C_i^t\}}{\min} \lim_{T \to \infty} \frac{1}{T} \sum_{t=0}^{T-1} \sum_{i \in \mathcal{I}} G(P_i^t) \quad (13a)$$

s. t. $\quad C_i^{\min} \leq C_i^t \leq C_i^{\max}, \forall i, t \quad (13b)$

$$C_i^{t+1} = C_i^t + P_i^t - P_{c,i} - \sum_{k \in \mathcal{K}} \mathrm{tr}(\mathbf{B}_i \mathbf{X}_k^t), \forall i, t \quad (13c)$$

$$P_{b,i}^{\min} \leq P_i^t - P_{c,i} - \sum_{k \in \mathcal{K}} \mathrm{tr}(\mathbf{B}_i \mathbf{X}_k^t) \leq P_{b,i}^{\max}, \forall i, t \quad (13d)$$

$$-P_{c,i} \leq \sum_{k \in \mathcal{K}} \mathrm{tr}(\mathbf{B}_i \mathbf{X}_k^t) \leq P_{g,i}^{\max} - P_{c,i}, \forall i, t \quad (13e)$$

$$\boldsymbol{\Gamma}_k^t \succeq \mathbf{0}, \quad \mathbf{X}_k^t \succeq \mathbf{0}, \quad \tau_k^t \geq 0, \forall k, t. \quad (13f)$$

The constraints (13a)–(13e) are all linear, and SINR constraints (10g) become a set of convex SDP constraints in (13f). As the objective function is already convex, the problem (13) is a convex problem. Note that a solution to (13) is a control policy that determines the sequence of feasible control decisions $\{\mathbf{X}_k^t, P_i^t, C_i^t\}$ to be used. Let G^* denote the value of the objective in (13) under an optimal control policy.

Although (13) becomes convex after judicious reformulation, it is still difficult to solve since we aim to minimize the average total cost over an infinite time horizon. In particular, the battery energy level relations in (13c) couple the optimization variables over the infinite time horizon. This renders the problem intractable for traditional solvers such as dynamic programming.

By recognizing that (13c) can be viewed as an energy queue recursion, we next apply the time decoupling technique to turn (13) into a tractable form [19], [20]. For the queue of C_i^t, the arrival and departure are P_i^t and $P_{c,i} + \sum_{k \in \mathcal{K}} \text{tr}(\mathbf{B}_i \mathbf{X}_k^t)$, respectively, per slot t. Over the infinite time horizon, the time-averaging rate of arrival and departure are given by $\lim_{T \to \infty} \frac{1}{T} \sum_{t=0}^{T-1} P_i^t$ and $P_{c,i} + \lim_{T \to \infty} \frac{1}{T} \sum_{t=0}^{T-1} \sum_{k \in \mathcal{K}} \text{tr}(\mathbf{B}_i \mathbf{X}_k^t)$, respectively. Define the following expected values:

$$\mathbb{E}\left[\sum_{i \in \mathcal{I}} G(P_i^t)\right] := \lim_{T \to \infty} \frac{1}{T} \sum_{t=0}^{T-1} \sum_{i \in \mathcal{I}} G(P_i^t) \qquad (14)$$

$$\mathbb{E}\left[P_i^t\right] := \lim_{T \to \infty} \frac{1}{T} \sum_{t=0}^{T-1} P_i^t \qquad (15)$$

$$\mathbb{E}\left[\sum_{k \in \mathcal{K}} \text{tr}(\mathbf{B}_i \mathbf{X}_k^t)\right] := \lim_{T \to \infty} \frac{1}{T} \sum_{t=0}^{T-1} \sum_{k \in \mathcal{K}} \text{tr}(\mathbf{B}_i \mathbf{X}_k^t) \qquad (16)$$

where the expectations are taken over all sources of randomness. These expectations exist due to the stationarity of $\{\mathbf{e}^t, \alpha^t, \beta^t\}$.

Now consider the following problem

$$\tilde{G}^* := \min_{\{P_i^t, \mathbf{\Gamma}_k^t, \mathbf{X}_k^t, \tau_k^t\}} \mathbb{E}\left[\sum_{i \in \mathcal{I}} G(P_i^t)\right] \qquad (17a)$$

$$\text{s. t.} \quad \mathbb{E}\left[P_i^t\right] = P_{c,i} + \mathbb{E}\left[\sum_{k \in \mathcal{K}} \text{tr}(\mathbf{B}_i \mathbf{X}_k^t)\right], \, \forall i \qquad (17b)$$

$$(13\text{d}) - (13\text{f}). \qquad$$

It can be shown that (17) is a relaxed version of (13). Specifically, any feasible solution of (13) also satisfies the constraints in (17). To see this, consider any policy that satisfies (13b) and (13c). Then summing equations in (13c) over all $t \in \mathcal{T}$ under such a policy yields: $C_i^T - C_i^0 = \sum_{t=0}^{T-1} [P_i^t - P_{c,i} - \sum_{k \in \mathcal{K}} \text{tr}(\mathbf{B}_i \mathbf{X}_k^t)]$. Since both C^T and C^0 are bounded due to (13b), dividing both sides by T and taking limits as $T \to \infty$, yields $\mathbb{E}[P_i^t] = P_{c,i} + \mathbb{E}[\sum_{k \in \mathcal{K}} \text{tr}(\mathbf{B}_i \mathbf{X}_k^t)]$. It is then clear that any feasible policy for (13) is also feasible for (17). As a result, the optimal value of (17) cannot exceed that of (13); that is, $\tilde{G}^* \leq G^*$.

Note that the time coupling constraint (13c) has been relaxed in problem (17), which then becomes easier to solve.

Specifically, it can be shown that the optimal solution to (17) can be achieved by[2] a stationary, randomized control policy that chooses control actions $\{\mathbf{X}_k^t, P_i^t\}$ every slot purely as a function (possibly randomized) of the current $\{\mathbf{e}^t, \alpha^t, \beta^t\}$ and independent of the battery energy levels C_i^t. We next develop a stochastic dual subgradient solver for (17), which under proper initialization can provide an asymptotically optimal solution to (13).

B. Stochastic Dual Subgradient Approach

Let $\mathcal{F}^t$ denote the set of $\{\mathbf{X}_k^t, \tau_k^t, P_i^t\}$ satisfying constraints (13d)–(13f) per t. Let λ_i, denote the Lagrange multipliers associated with the constraints (17b). With the convenient notation $\mathbf{Z}^t := \{\mathbf{X}_k^t, \tau_k^t, P_i^t\}$, $\mathbf{Z} := \{\mathbf{Z}^t, \forall t\}$, and $\boldsymbol{\lambda} := \{\lambda_i, \forall i\}$, the partial Lagrangian function of (17) is

$$L(\mathbf{Z}, \boldsymbol{\lambda}) :=$$
$$\mathbb{E}\left[\sum_i G(P_i^t)\right] + \sum_i \lambda_i \left(\mathbb{E}\left[P_i^t\right] - P_{c,i} - \mathbb{E}\left[\sum_{k \in \mathcal{K}} \text{tr}(\mathbf{B}_i \mathbf{X}_k^t)\right]\right). \qquad (18)$$

while the Lagrange dual function is given by

$$D(\boldsymbol{\lambda}) := \min_{\{\mathbf{Z}^t \in \mathcal{F}^t\}_t} L(\mathbf{Z}, \boldsymbol{\lambda}), \qquad (19)$$

and the dual problem of (17) is: $\max_{\boldsymbol{\lambda}} D(\boldsymbol{\lambda})$.

For the dual problem, we can resort to a standard subgradient method to obtain the optimal $\boldsymbol{\lambda}^*$. This amounts to running the iterations

$$\lambda_i(j+1) = \lambda_i(j) + \mu g_{\lambda_i}(j), \, i = 1, \ldots, I \qquad (20)$$

where j is the iteration index and $\mu > 0$ is an appropriate stepsize. The subgradient $\mathbf{g}(j) := [g_{\lambda_i}(j), \forall i]$ can then be expressed as

$$g_{\lambda_i}(j) = \mathbb{E}[P_i^t(j)] - P_{c,i} - \mathbb{E}\left[\sum_{k \in \mathcal{K}} \text{tr}(\mathbf{B}_i \mathbf{X}_k^t(j))\right] \qquad (21)$$

where $\mathbf{X}_k^t(j)$ and $P_i^t(j)$ are given by

$$\{\mathbf{X}_k^t(j), P_i^t(j)\} \in \arg\min_{\{\mathbf{X}_k^t, P_i^t\} \in \mathcal{F}^t} \sum_{i \in \mathcal{I}} \left[G(P_i^t)\right.$$
$$\left. + \lambda_i(j)\left(P_i^t - P_{c,i} - \sum_{k \in \mathcal{K}} \text{tr}(\mathbf{B}_i \mathbf{X}_k^t)\right)\right]. \qquad (22)$$

Since $\mathcal{F}^t$ is a convex set while the objective is a convex function of $\{\mathbf{X}_k^t, P_i^t\}$, the minimization problem in (22) is a convex program that is efficiently solvable to obtain the optimal $\{\mathbf{X}_k^t(j), P_i^t(j)\}$.

When a constant stepsize μ is adopted, the subgradient iterations (20) are guaranteed to converge to a neighborhood of the optimal $\boldsymbol{\lambda}^*$ for the dual problem from any initial $\boldsymbol{\lambda}(0)$. The size of the neighborhood is proportional to the stepsize μ. In fact, if we adopt a sequence of non-summable diminishing stepsizes

---

[2]The proof follows from the framework in [21] and is omitted for brevity.

Algorithm 1. Virtual-Queue based Online Control (VQOC)

1: Initialize with a proper $\mathbf{Q}^0 = \{Q_i^0, \forall i\}$
2: Repeat online $t = 1, 2, \ldots$
   With $\mathbf{Q}^t, \{\mathbf{e}^t, \alpha^t, \beta^t\}$ available per slot t, solve the problem in (22) with $\lambda_i \equiv \mu Q_i^t, \forall i$, to obtain $\{P_i^t(\mathbf{Q}^t), \mathbf{X}_k^t(\mathbf{Q}^t)\}$, and then perform the corresponding online beamforming and battery-charging, power-buying/selling operations
3: Update the virtual queue $\mathbf{Q}^{t+1}$ via (24) for all i

---

satisfying $\lim_{j \to \infty} \mu(j) = 0$ and $\sum_{j=0}^{\infty} \mu(j) = \infty$, then the iterations (20) converge to the exact $\boldsymbol{\lambda}^*$ as $j \to \infty$ [25]. Since (17) is convex, the duality gap is zero, and convergence to $\boldsymbol{\lambda}^*$ can also yield the optimal solution to the primal problem (17).

A challenge associated with the subgradient iterations (20) is computing $\mathbb{E}[P_i^t(j)]$ and $\mathbb{E}[\sum_k \mathrm{tr}(\mathbf{B}_i \mathbf{X}_k^t(j))]$ per iterate. This amounts to performing high-dimensional integration over unknown (or known) joint distribution function; or approximately, computing the corresponding time-averages over an infinite time horizon. Such a requirement is impractical since the associated computational complexity could be prohibitively high. To bypass this impasse, we will rely on a stochastic subgradient approach. Specifically, dropping $\mathbb{E}$ from (20), we propose the following iteration

$$\hat{\lambda}_i^{t+1} = \hat{\lambda}_i^t + \mu \left[P_i^t(\hat{\lambda}^t) - P_{c,i} - \sum_k \mathrm{tr}(\mathbf{B}_i \mathbf{X}_k^t(\hat{\lambda}^t)) \right] \quad (23)$$

where $\{\hat{\lambda}_i^t\}_t$ indicate the stochastic estimates of those in (20), and $P_i^t(\hat{\lambda}^t)$, $\mathbf{X}_k^t(\hat{\lambda}^t)$ are obtained by solving (22) with $\lambda_i(j)$ replaced by $\hat{\lambda}_i^t, \forall i$.

Note that t denotes both iteration and slot indices. In other words, the update (23) is an *online* approximation algorithm based on the *instantaneous* decisions $\{P_i^t(\hat{\lambda}^t), \mathbf{X}_k^t(\hat{\lambda}^t)\}$ per slot t. This stochastic approach is made possible due to the decoupling of optimization variables across time in (17). Convergence of online iterations (23) to the optimal $\boldsymbol{\lambda}^*$ can be established in different senses; see [21], [26]–[29]. Due to the zero-duality gap, the companion $\{P_i^t(\hat{\lambda}^t), \mathbf{X}_k^t(\hat{\lambda}^t)\}$ will also converge to the optimal policy of (17).

C. Virtual-Queue based Control Algorithm

Based on the stochastic iterations (23), we next develop a virtual-queue based online control (VQOC) algorithm for (17). With $\mathbf{Q}^t := \{Q_i^t := \hat{\lambda}_i^t/\mu, \ i = 1, \ldots, I\}$, it is clear that

$$Q_i^{t+1} = Q_i^t + P_i^t(\mathbf{Q}^t) - P_{c,i} - \sum_k \mathrm{tr}(\mathbf{B}_i \mathbf{X}_k^t(\mathbf{Q}^t)) \quad (24)$$

where $P_i^t(\mathbf{Q}^t) := P_i^t(\mu \mathbf{Q}^t) = P_i^t(\hat{\lambda}^t)$, and $\mathbf{X}_k^t(\mathbf{Q}^t) := \mathbf{X}_k^t(\hat{\lambda}^t)$.

Note that Q_i^t in (24) obeys the same dynamical equation as the SoC in (13c); hence, it can be seen as a virtual energy queue for the i-th BS. Unlike real queues, the value of Q_i^t is allowed to be negative. Based on such virtual queues, we propose the following VQOC algorithm at the central scheduler.

For Algorithm 1, the information of harvested energy $\{\mathbf{e}^t\}$ at the BSs can be collected by each cluster's central unit through cellular backhaul links. The energy pricing information $\{\alpha^t, \beta^t\}$

is available via smart meters installed at BSs, and the grid-deployed communication/control links connecting them. The channel estimates $\hat{\mathbf{h}}_k^t$ can be obtained by limited-feedback channels specified in the current and future cellular standards. In a nutshell, the communication overhead associated with the proposed algorithm is affordable in next-generation smart-grid power CoMP systems. The computational complexity with the proposed VQOC algorithm is also low. Specifically, the interior-point method can be employed to solve the convex problem (22) yielding $\{P_i^t(\mathbf{Q}^t), \mathbf{X}_k^t(\mathbf{Q}^t)\}$ with a complexity $\mathcal{O}((MI)^{3.5})$ per slot t [30]. Update of $\mathbf{Q}^{t+1}$ in (24) incurs only linear complexity $\mathcal{O}(MI)$.

The VQOC algorithm is essentially the stochastic subgradient solver (23). In the next section, we will rigorously establish that the proposed algorithm can asymptotically yield an optimal solution of (17). Interestingly, by exploiting the connection between Q_i^t and C_i^t, we will also show that the VQOC approach with proper initialization also yields a solution to (13), or, to the original problem (10).

IV. PERFORMANCE GUARANTEES

To arrive at our main claim, we first establish the asymptotic optimality of the proposed VQOC algorithm.

A. Asymptotic Optimality

Relying on the so-called Lyapunov optimization technique in [19]–[21], we can formally establish that:

Lemma 1: If $\{\mathbf{e}^t, \alpha^t, \beta^t\}$ are i.i.d. over slots, then the time-averaging cost under the proposed VQOC algorithm satisfies

$$\lim_{T \to \infty} \frac{1}{T} \sum_{t=0}^{T-1} \mathbb{E} \left[\sum_i G(P_i^t(\mathbf{Q}^t)) \right] \le G^* + \mu M$$

where the constant $M := \frac{1}{2} \sum_i (\max\{P_{b,i}^{\max}, -P_{b,i}^{\min}\})^2$, and G^* is the optimal value of (13) under any feasible control algorithm, even if that relies on knowing future random realizations.

Proof: From the evolutions in (24), we have

$$(Q_i^{t+1})^2 = [Q_i^t + P_i^t(\mathbf{Q}^t) - P_{c,i} - \sum_k \mathrm{tr}(\mathbf{B}_i \mathbf{X}_k^t(\mathbf{Q}^t))]^2$$

$$= (Q_i^t)^2 + 2Q_i^t[P_i^t(\mathbf{Q}^t) - P_{c,i} - \sum_k \mathrm{tr}(\mathbf{B}_i \mathbf{X}_k^t(\mathbf{Q}^t))]$$

$$+ [P_i^t(\mathbf{Q}^t) - P_{c,i} - \sum_k \mathrm{tr}(\mathbf{B}_i \mathbf{X}_k^t(\mathbf{Q}^t))]^2$$

$$\le (Q_i^t)^2 + 2Q_i^t[P_i^t(\mathbf{Q}^t) - P_{c,i} - \sum_k \mathrm{tr}(\mathbf{B}_i \mathbf{X}_k^t(\mathbf{Q}^t))]$$

$$+ (\max\{P_{b,i}^{\max}, -P_{b,i}^{\min}\})^2$$

where the last inequality holds due to (13d).

Considering now the Lyapunov function $V(\mathbf{Q}^t) := \frac{1}{2} \sum_i (Q_i^t)^2$, it readily follows that

$$\triangle V(\mathbf{Q}^t) := V(\mathbf{Q}^{t+1}) - V(\mathbf{Q}^t)$$

$$\le \sum_i \{Q_i^t[P_i^t(\mathbf{Q}^t) - P_{c,i} - \sum_k \mathrm{tr}(\mathbf{B}_i \mathbf{X}_k^t(\mathbf{Q}^t))]\} + M.$$

Taking expectations and adding $\frac{1}{\mu} \mathbb{E}[\sum_i G(P_i^t(\mathbf{Q}^t))]$ to both sides, we arrive at

$$\mathbb{E}[\triangle V(\mathbf{Q}^t)] + \frac{1}{\mu}\mathbb{E}[\sum_i G(P_i^t(\mathbf{Q}^t))]$$

$$\leq M + \frac{1}{\mu}\left(\mathbb{E}[\sum_i G(P_i^t(\mathbf{Q}^t))] + \sum_i \left\{\mu Q_i^t\left(\mathbb{E}[P_i^t(\mathbf{Q}^t)]\right.\right.\right.$$

$$\left.\left.\left.- P_{c,i} - \mathbb{E}[\sum_k \text{tr}(\mathbf{B}_i \mathbf{X}_k^t(\mathbf{Q}^t))]\right)\right\}\right)$$

$$= M + \frac{1}{\mu}L(\mathbf{Z}(\mu\mathbf{Q}^t), \mu\mathbf{Q}^t)$$

$$= M + \frac{1}{\mu}D(\mu\mathbf{Q}^t)$$

$$\leq M + \frac{1}{\mu}\tilde{G}^*$$

where we used the definition of $L(\mathbf{Z}, \boldsymbol{\lambda})$ in (18); $\mathbf{Z}(\mu\mathbf{Q}^t)$ denotes the optimal primal variable set given by (22) for $\boldsymbol{\lambda} = \mu\mathbf{Q}^t$ (hence, $L(\mathbf{Z}(\mu\mathbf{Q}^t), \mu\mathbf{Q}^t) = D(\mu\mathbf{Q}^t)$); $\tilde{G}^*$ denotes the optimal value for problem (17); and the last inequality is due to the weak duality: $D(\boldsymbol{\lambda}) \leq \tilde{G}^*, \forall\boldsymbol{\lambda}$.

Summing over all t, we then have

$$\sum_{t=0}^{T-1}\mathbb{E}[\triangle V(\mathbf{Q}^t)] + \frac{1}{\mu}\sum_{t=0}^{T-1}\mathbb{E}[\sum_i G(P_i^t(\mathbf{Q}^t))]$$

$$= \mathbb{E}[V(\mathbf{Q}^T)] - V(\mathbf{Q}^0) + \frac{1}{\mu}\sum_{t=0}^{T-1}\mathbb{E}[\sum_i G(P_i^t(\mathbf{Q}^t))]$$

$$\leq T(M + \frac{1}{\mu}\tilde{G}^*)$$

which leads to

$$\frac{1}{T}\sum_{t=0}^{T-1}\mathbb{E}[\sum_i G(P_i^t(\mathbf{Q}^t))] \leq \tilde{G}^* + \mu\left(M + \frac{V(\mathbf{Q}^0)}{T}\right)$$

$$\leq G^* + \mu\left(M + \frac{V(\mathbf{Q}^0)}{T}\right).$$

The lemma follows by taking the limit $T \to \infty$. $\blacksquare$

Lemma 1 asserts that the proposed VQOC algorithm converges to a region with an optimality gap smaller than μM, which vanishes as the stepsize $\mu \to 0$. The proof follows the lines of the Lyapunov technique in e.g., [21]. Yet, slightly different from [21], here the Lagrange dual theory is utilized to simplify the arguments.

B. Feasibility Guarantee

We have shown that the VQOC iteration can achieve a near-optimal objective value for (13). However, since the proposed algorithm is based on a solver for the relaxed (17), it is not guaranteed that the resultant dynamic control policy is a feasible one for (13). In the sequel, we will establish that the VQOC in fact can yield a feasible policy for (13) when it is properly initialized. To this end, we first show the following lemma.

Lemma 2: If $\bar{\alpha} := \max\{\alpha^t, \forall t\}$ and $\underline{\beta} := \min\{\beta^t, \forall t\}$, the battery (dis-)charging amounts $P_{b,i}^t$ under the VQOC algorithm obey: i) $P_{b,i}^t(\mathbf{Q}^t) = P_{b,i}^{\min}$, if $Q_i^t > \frac{-\underline{\beta}}{\mu}$; and ii) $P_{b,i}^t(\mathbf{Q}^t) = P_{b,i}^{\max}$, if $Q_i^t < \frac{-\bar{\alpha}}{\mu}$.

Proof: Since $P_{b,i}^t = P_i^t - P_{c,i} - \sum_{k\in\mathcal{K}}\text{tr}(\mathbf{B}_i\mathbf{X}_k^t)$, per slot t we have

$$\{\mathbf{X}_k^t(\mathbf{Q}^t), P_{b,i}^t(\mathbf{Q}^t)\} \in \arg\min_{\{\mathbf{X}_k^t, P_{b,i}^t\}\in\mathcal{F}^t}\sum_i\left[G(P_{b,i}^t + P_{c,i}\right.$$

$$\left.+ \sum_{k\in\mathcal{K}}\text{tr}(\mathbf{B}_i\mathbf{X}_k^t)) + \mu Q_i^t P_{b,i}^t\right].$$

Consider the following two cases [cf. (9)]

i) If $P_{b,i}^t(\mathbf{Q}^t) + P_{c,i} + \sum_k\text{tr}(\mathbf{B}_i\mathbf{X}_k^t(\mathbf{Q}^t)) \geq E_i^t$, then $G(P_{b,i}^t(\mathbf{Q}^t) + P_{c,i} + \sum_k\text{tr}(\mathbf{B}_i\mathbf{X}_k^t(\mathbf{Q}^t))) = \alpha^t\left(P_{b,i}^t(\mathbf{Q}^t) + P_{c,i} + \sum_k\text{tr}(\mathbf{B}_i\mathbf{X}_k^t(\mathbf{Q}^t)) - E_i^t\right)$. It is easy to see that we must have

$$P_{b,i}^t(\mathbf{Q}^t) = \begin{cases} P_{b,i}^{\min}, & \text{if } \mu Q_i^t + \alpha^t > 0 \\ P_{b,i}^{\max}, & \text{if } \mu Q_i^t + \alpha^t < 0. \end{cases}$$

ii) If $P_{b,i}^t(\mathbf{Q}^t) + P_{c,i} + \sum_k\text{tr}(\mathbf{B}_i\mathbf{X}_k^t(\mathbf{Q}^t)) < E_i^t$, then $G(P_{b,i}^t(\mathbf{Q}^t) + P_{c,i} + \sum_k\text{tr}(\mathbf{B}_i\mathbf{X}_k^t(\mathbf{Q}^t))) = \beta^t\left(P_{b,i}^t(\mathbf{Q}^t) + P_{c,i} + \sum_k\text{tr}(\mathbf{B}_i\mathbf{X}_k^t(\mathbf{Q}^t)) - E_i^t\right)$; and we similarly arrive at

$$P_{b,i}^t(\mathbf{Q}^t) = \begin{cases} P_{b,i}^{\min}, & \text{if } \mu Q_i^t + \beta^t > 0 \\ P_{b,i}^{\max}, & \text{if } \mu Q_i^t + \beta^t < 0. \end{cases}$$

Combining cases i) and ii), we deduce that per slot t, if $\mu Q_i^t > \max\{-\alpha^t, -\beta^t\} = -\beta^t$, then $P_{b,i}^t(\mathbf{Q}^t) = P_{b,i}^{\min}$. This implies that if $Q_i^t > \frac{-\beta}{\mu}$, we must have $P_{b,i}^t(\mathbf{Q}^t) = P_{b,i}^{\min}$. Similarly, if $\mu Q_i^t < \min\{-\alpha^t, -\beta^t\} = -\alpha^t$, then $P_{b,i}^t(\mathbf{Q}^t) = P_{b,i}^{\max}$, which is guaranteed whenever $Q_i^t < \frac{-\bar{\alpha}}{\mu}$. $\blacksquare$

Remark 1: Lemma 2 reveals partial characteristics of the dynamic VQOC policy. Specifically, when the virtual energy queue is large enough, the battery must be discharged as much as possible; i.e., $P_{b,i}^t(\mathbf{Q}^t) = P_{b,i}^{\min}$. On the other hand, when the virtual queue is small (negative) enough, the battery must be charged as much as possible; i.e., $P_{b,i}^t(\mathbf{Q}^t) = P_{b,i}^{\max}$. Alternatively, such results can be justified by the economic interpretation of the Lagrange multipliers [cf. (23) and (18)]. Specifically, $\hat{\lambda}_i^t$ can be viewed as the stochastic instantaneous charging price. For high prices $\hat{\lambda}_i^t = \mu Q_i^t > -\beta^t$, the VQOC dictates the full discharge $P_{b,i}^t(\mathbf{Q}^t) = P_{b,i}^{\min}$. Conversely, the battery units can afford full charge if the price is low; i.e., $\hat{\lambda}_i^t = \mu Q_i^t < -\alpha^t$. It is worth stressing that a closed-form solution of $P_{b,i}^t$ is generally not available when $\hat{\lambda}_i^t \in [-\alpha^t, -\beta^t]$, where one must resort to solving (22) numerically.

Leveraging this intuition, we will establish the following lemma on the virtual queue bounds, which is useful for our main theorem. Suppose $\gamma := 1/\min\{C_i^{\max} - C_i^{\min} + P_{b,i}^{\min} - P_{b,i}^{\max}, \forall i\} > 0$ holds.

Lemma 3: If the step size satisfies $\mu \geq \underline{\mu} := \gamma(\bar{\alpha} - \underline{\beta})$, then the VQOC guarantees the virtual queue $Q_i^t \in \left[-\frac{\bar{\alpha}}{\mu} + P_{b,i}^{\min}, C_i^{\max} - C_i^{\min} - \frac{\bar{\alpha}}{\mu} + P_{b,i}^{\min}\right]$ for all i and t.

Proof: The proof proceeds by induction. First, set $Q_0^t \in \left[-\frac{\bar{\alpha}}{\mu} + P_{b,i}^{\min}, C_i^{\max} - C_i^{\min} - \frac{\bar{\alpha}}{\mu} + P_{b,i}^{\min}\right]$, and suppose that

this holds for all $\{Q_i^t\}_i$ at slot t. We will show the bounds hold for $\{Q_i^{t+1}\}_i$ as well in subsequent instances.

c1) If $Q_i^t \in (\frac{-\beta}{\mu}, C_i^{\max} - C_i^{\min} - \frac{\bar{\alpha}}{\mu} + P_{b,i}^{\min}]$, it follows from Lemma 2 that $Q_i^{t+1} = Q_i^t + P_{b,i}^{\min} \in (-\frac{\bar{\alpha}}{\mu} + P_{b,i}^{\min},$ $C_i^{\max} - C_i^{\min} - \frac{\bar{\alpha}}{\mu} + P_{b,i}^{\min})$ holds provided that $\frac{-\bar{\alpha}}{\mu} < \frac{-\beta}{\mu}$ and $P_{b,i}^{\min} < 0$.

c2) If $Q_i^t \in [-\frac{\bar{\alpha}}{\mu}, \frac{-\beta}{\mu}]$, then $Q_i^{t+1} = Q_i^t + P_{b,i}^t(\mathbf{Q}^t) \in [Q_i^t + P_{b,i}^{\min}, Q_i^t + P_{b,i}^{\max}] \subseteq [-\frac{\bar{\alpha}}{\mu} + P_{b,i}^{\min}, \frac{-\beta}{\mu} + P_{b,i}^{\max}] \subseteq [-\frac{\bar{\alpha}}{\mu} + P_{b,i}^{\min}, C_i^{\max} - C_i^{\min} - \frac{\bar{\alpha}}{\mu} + P_{b,i}^{\min}]$, which holds using that $\mu \geq \underline{\mu}$.

c3) If $Q_i^t \in [-\frac{\bar{\alpha}}{\mu} + P_{b,i}^{\min}, -\frac{\bar{\alpha}}{\mu})$, then by Lemma 2 we have $Q_i^{t+1} = Q_i^t + P_{b,i}^{\max} \in [-\frac{\bar{\alpha}}{\mu} + P_{b,i}^{\min} + P_{b,i}^{\max}, -\frac{\bar{\alpha}}{\mu} + P_{b,i}^{\max}) \subseteq (-\frac{\bar{\alpha}}{\mu} + P_{b,i}^{\min}, C_i^{\max} - C_i^{\min} - \frac{\bar{\alpha}}{\mu} + P_{b,i}^{\min})$, where the last step follows from the facts $P_{b,i}^{\max} > 0$, $\frac{-\bar{\alpha}}{\mu} < \frac{-\beta}{\mu}$, and case c2). ∎

Consider now the linear mapping

$$C_i^t = Q_i^t + \frac{\bar{\alpha}}{\mu} + C_i^{\min} - P_{b,i}^{\min}, \quad i = 1, \ldots, I. \qquad (25)$$

It can be readily seen from Lemma 3 that $C_i^{\min} \leq C_i^t \leq C_i^{\max}$ holds for all i and t; i.e, (13b) is always satisfied under the VQOC. In addition, the battery (dis)charging dynamics (13c) are met since they coincide with those of the virtue queues (24). Hence, the proposed VQOC scheme yields a feasible dynamic control policy for the problem (13).

C. Main Theorem

Based on Lemmas 1 and 3, it is now possible to arrive at our main result.

Theorem 1: If we set $Q_i^0 = C_i^0 - \frac{\bar{\alpha}}{\mu} + P_{b,i}^{\min} - C_i^{\min}, \forall i$, and select a stepsize $\mu \geq \underline{\mu}$, then the proposed VQOC yields a feasible dynamic control scheme for (17), which is asymptotically optimal in the sense that

$$\lim_{T \to \infty} \frac{1}{T} \sum_{t=0}^{T-1} \mathbb{E}[\sum_i G(P_i^t(\mathbf{Q}^t))] \leq G^* + \mu M$$

where $\underline{\mu} := (\bar{\alpha} - \underline{\beta})/ \min \left\{ C_i^{\max} - C_i^{\min} + P_{b,i}^{\min} - P_{b,i}^{\max}, \forall i \right\}$, and $M := \frac{1}{2} \sum_i (\max\{P_{b,i}^{\max}, -P_{b,i}^{\min}\})^2$.

Clearly, the minimum optimality gap (regret) between the VQOC and the offline scheduling is given by

$$\underline{\mu} M = \frac{1}{2} \gamma (\bar{\alpha} - \underline{\beta}) \sum_i (\max\{P_{b,i}^{\max}, -P_{b,i}^{\min}\})^2.$$

Asymptotically (sub)optimal solution can be attained if we have very small price difference $(\bar{\alpha} - \underline{\beta})$, or γ incurred by e.g., very large battery capacities $\{C_i^{\max}\}_i$. This makes sense intuitively because when all BS batteries have large capacity, the upper bounds in (13b) are loose. With proper initialization, the VQOC using any μ will be feasible for (13). We can then reach the optimal G^* as close as possible. In addition, let us consider a

homogeneous setup, which is common in practice: $-P_{b,i}^{\min} = P_{b,i}^{\max} = \eta C_i^{\max} = \eta \tilde{C}$ and $C_i^{\min} = 0$ for all i. Then it can be seen that $\underline{\mu} M = \frac{1}{2} I \tilde{C}(\bar{\alpha} - \underline{\beta}) \frac{\eta^2}{1 - 2\eta}$ which is an increasing function for $\eta \in (0, \frac{1}{2})$. Hence, a small (dis)charging efficiency η can also result in a near optimal scheduling under the VQOC.

Problem (13) is indeed an SDP relaxation of the original problem (10). If the obtained solution for (13) satisfies the condition rank$(\mathbf{X}_k^{t*}) = 1, \forall k, t$, then it clearly yields the optimal beamforming vectors $\mathbf{w}_k^{t*}$ of (10) as the (scaled) eigenvector with respect to the only positive eigenvalue of $\mathbf{X}_k^{t*}$. Fortunately, it was shown in [31, Them. 1] that the S-procedure based SDP in (13) always returns a rank-one optimal solution $\mathbf{X}_k^{t*}, \forall k, t$, when the uncertainty bounds ϵ_k^t are sufficiently small. If ϵ_k is large, existence of rank-one optimal solutions for (13) cannot be provably guaranteed. In this case, a randomized rounding strategy [32] is often adopted to obtain vectors $\mathbf{w}_k^{t*}$ from $\mathbf{X}_k^{t*}$ that nicely approximates the solution of the original problem (10). Even though no proof is available to ensure a rank-one solution when ϵ_k is large, it has been extensively observed in simulations that the SDP relaxation always yields a rank-one optimal solution [31]. This confirms the view that the asymptotically optimal beamforming vectors for the original problem (10) will be obtained by our approach with high probability.

V. NUMERICAL TESTS

In this section, simulated tests are presented to demonstrate the efficacy of the proposed approach and justify our analytical claims. The Matlab-based modeling package CVX 2.1 [30] and SDPT3 [33] are used to solve the resulting optimization problem (22). All numerical tests are implemented on a PC with eight 3.40 GHz Intel cores and 32 GB RAM.

Two configurations of the considered CoMP network are tested: (S1) $I = 2$ BSs each with $M = 2$ transmit antennas, and $K = 10$ mobile users (small size); and (S2) $I = 4$ BSs each with $M = 2$ transmit antennas, and $K = 15$ mobile users (large size).

Under (S1), the purchase price α^t is generated from a folded normal distribution; that is, $\alpha^t = |x|$ with $x \sim \mathcal{N}(3, 3)$. The selling price is set to $\beta^t = r\alpha^t$ with $r = 0.9$. Samples of the harvested energy $\{E_i^t\}_{i,t}$ are generated from a Weibull distributed wind speed and wind-speed-to-wind-power mapping. The wind power capacity of each farm is $E^{\max} = 10$ kW, unless stated otherwise [34]. For (S2), the purchase price α^t is obtained from the hourly electricity prices in New York from Jan. 1 to Jan. 30, 2015 [35]. The harvested energy $\{E_i^t\}$ is a scaled version of the hourly wind generation connected to the PJM grids during the same periods [36]. The limits of $P_{g,i}, C_i$, $P_{b,i}$ and the initial SoC C_i^0 are listed in Table I. Following the Samsung energy storage solutions [37], battery capacity $C^{\max}$ is set to 50 kW in (S1), and 100 kW in (S2) for all BSs. The estimated channel state $\hat{\mathbf{h}}_k^t$ is a zero-mean complex-Gaussian random variable with unit variance, while the maximum prediction error is $(\epsilon_k^t)^2 = 0.1$. Finally, the stepsize is chosen as $\mu \equiv \underline{\mu}$ [cf. Theorem 1].

The proposed approach is compared with two baseline algorithms including VQOC without RES (no-RES), and greedy scheme that aims at minimizing the *instantaneous* transaction

TABLE I
GENERATING CAPACITIES, BATTERY INITIAL ENERGY AND CAPACITY,
AND CHARGING LIMITS. ALL UNITS ARE kW

BS_i	$P_{g,i}^{\min}$	$P_{g,i}^{\max}$	$C_i^{\min}$	C_i^0	$P_{b,i}^{\min}$	$P_{b,i}^{\max}$	$P_{c,i}$
1	0	55	5	5	-10	10	10
2	0	50	5	5	-10	10	10
3	0	45	5	5	-10	10	10
4	0	40	5	5	-10	10	10

Fig. 3. Comparison of the average transaction cost (S1).
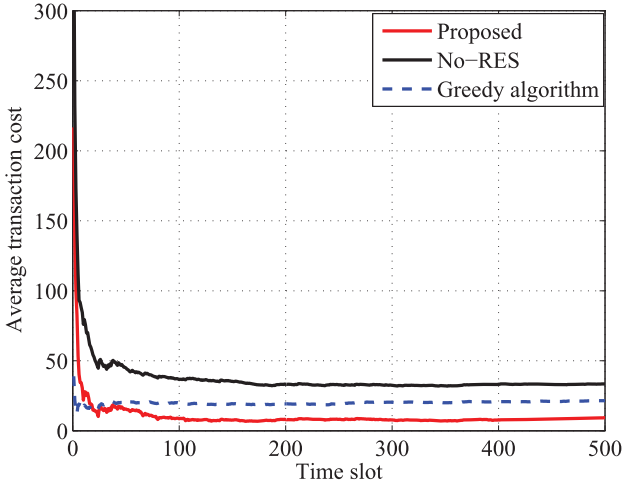
Fig. 4. Comparison of the average transaction cost (S2).

cost per time slot. For the greedy algorithm, instantaneous decisions $\{\mathbf{X}_k^t, \tau_k^t, P_i^t\}$ are obtained by solving the convex problem (13) per slot t with fixed $\{C_i^t\}_{i\in\mathcal{I}}$. Feasibility of the solutions across horizons is guaranteed by simply updating C_i^{t+1} via (13c). Note that all surplus or shortage energy must be traded per slot in order to minimize the instantaneous cost. Therefore, storage units essentially do not play a role since there is no (dis)charging activity. This makes the greedy scheme myopic and vulnerable to high future purchase prices.

In Figs. 3 and 4, the average transaction costs (13a) of the proposed VQOC, the no-RES schedule, and the greedy algorithm are compared for both (S1) and (S2). Note that the VQOC approach incurs the same computational complexity as the greedy algorithm. Clearly, within 500 iterations (time slots) VQOC converges to a transaction cost lower than the ones resulting from the no-RES schedule, and the greedy algorithm in Fig. 3. Intuitively, this is because the proposed VQOC can intelligently leverage the energy storage to hedge against future large losses while the greedy scheme cannot. The performance gain of the proposed approach is shown in Fig. 4 for the non i.i.d. case. When prices peak, considerable cost savings are obtained by the proposed algorithm that intelligently leverages stored energy in the battery with transactions. Specifically, more locally stored energy will be utilized to balance out the energy shortage when the purchase price α^t is high. Likewise, additional excess energy can be sold to the main grid with a high selling price β^t. The introduced transaction mechanism essentially confirms the advantage of the battery-deployed communication system design to mitigate the grid uncertainty.

The energy purchase prices α^t, selling prices β^t, Lagrangian multipliers $\hat{\lambda}_1^t$, as well as the real-time battery (dis)charging
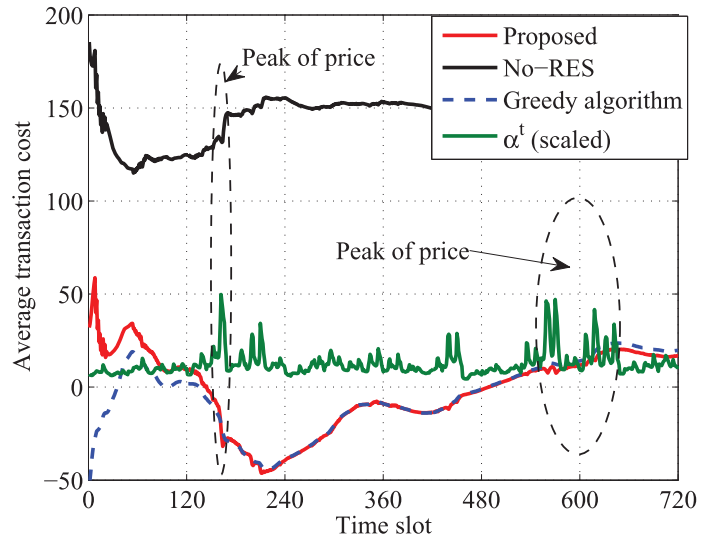
actions $P_{b,1}^t$ are shown in Fig. 5. It can be seen that we have $P_{b,1}^t = P_{b,1}^{\min}$ when $\hat{\lambda}_i^t > -\beta^t$ at $t = 1, 3, 5, 7, 8, 11$, while $P_{b,1}^t = P_{b,1}^{\max}$ when $\hat{\lambda}_i^t < -\alpha^t$ at $t = 2, 4, 6, 9, 10$. Such mapping relationships are also true for the slots $t > 12$ and $P_{b,2}^t$, which corroborate the assertion of Lemma 2. It is worth mentioning that the battery switching rate is in the time scale of the online scheduling, which can be in the order of (milli) seconds or even minutes depending on the system design requirements. For the sake of battery health and lifespan, it is desirable to control the charging and discharging switch frequency. To achieve this goal, we can simply impose a battery switching cost or constraint [10], or design and implement a two time scale scheduling approach where the battery can be operated in the slow time scale [38].

Figs. 6 and 7 demonstrate how the SoC's feasibility is affected by the stepsize μ. In Fig. 6, the SoC is always feasible ($C_1^{\min} \leq C_1^t \leq C_1^{\max}$) when $\mu = \underline{\mu}$. In contrast, if we choose $\mu = 0.5\underline{\mu}$ that does not satisfy the stepsize condition in Lemma 3, then $\bar{C}_1^t$ exceeds its upper bound very often as corroborated by Fig. 7.

The average transaction costs of the VQOC and greedy approaches with respect to the storage capacity $C^{\max}$ are depicted in Fig. 8. It can be seen that the VQOC's transaction cost deceases monotonically as $C^{\max}$ increases. This corroborates the result of Theorem 1 dictating that the optimality gap $\underline{\mu}M$, as well as the optimal value G^* is decreasing with $C^{\max}$. Note that as analyzed earlier, the greedy algorithm cannot benefit from the increase of the storage capacity,

Figs. 9 and 10 show the average cost with respect to the price ratio $r = \beta^t/\alpha^t$, where α^t is fixed. We studied two scenarios: i) small harvested wind power $E^{\max} = 10$ kW, and ii) a large one $E^{\max} = 15$ kW. Clearly, for both scenarios, the average cost of the VQOC decreases as r increases. This is because the optimality gap $\underline{\mu}M$ and the optimal value G^* are decreasing functions with respect to r.

Moreover, it is interesting to see that the greedy algorithm exhibits different performance in these two cases. When the
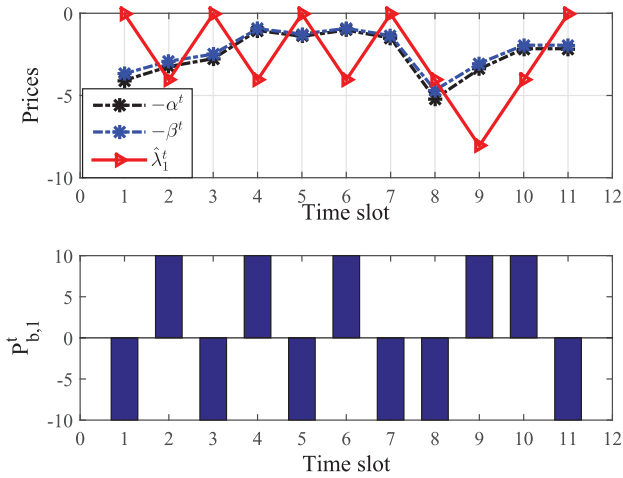
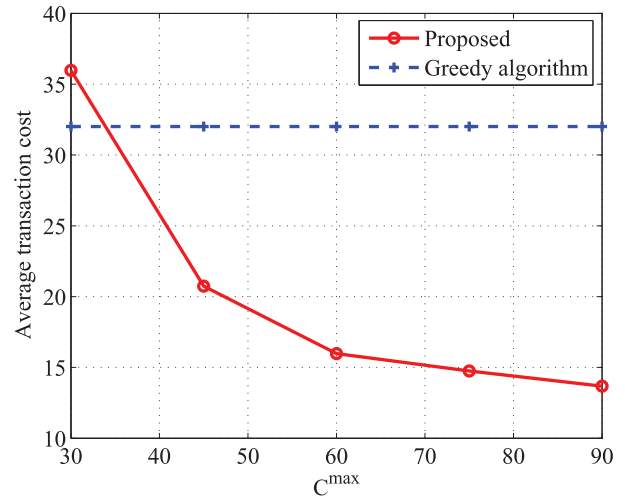Fig. 5. VQOC based power schedule of $P_{b,1}^t$ (S1).

Fig. 6. VQOC based power schedule of C_1^t (S1, $\mu = \underline{\mu}$).
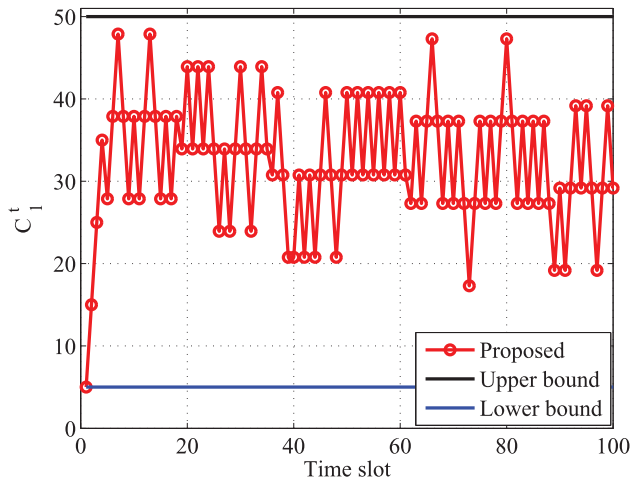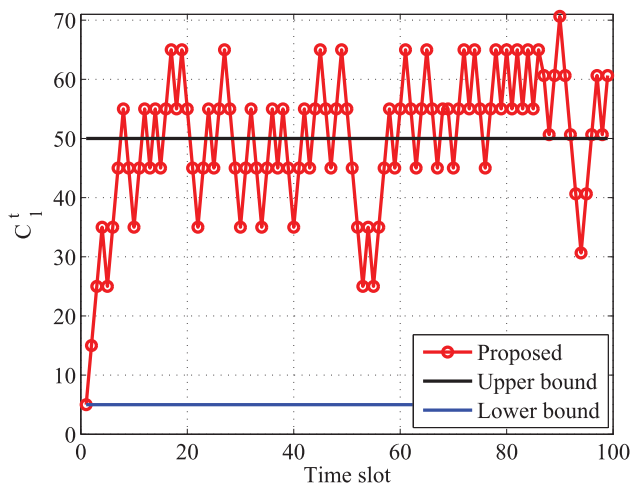

Fig. 7. VQOC based power schedule of C_1^t (S1, $\mu = 0.5\underline{\mu}$).

Fig. 8. Average transaction cost versus $C_1^{\max}$ (S1, $r = 0.9$).

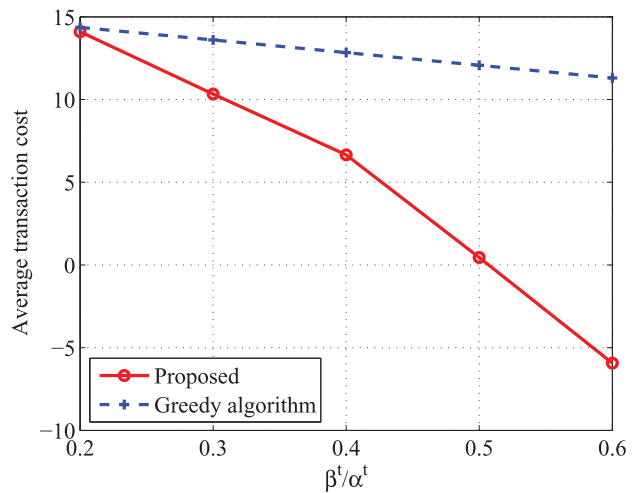Fig. 9. Average transaction cost versus $r = \beta^t/\alpha^t$ (S1).

Fig. 10. Average transaction cost versus $r = \beta^t/\alpha^t$ (S1, $E^{\max} = 15$).

wind power is small, most of the time greedy algorithm has to purchase shortage energy in order to support the CoMP's operation. As shown in Fig. 9, the average transaction cost is not affected by only increasing the selling price β^t in this case.

Conversely, by taking advantage of large harvested wind power, greedy algorithm can make more profits by selling the surplus with the increase of β^t. Hence, in Fig. 10 the average cost of
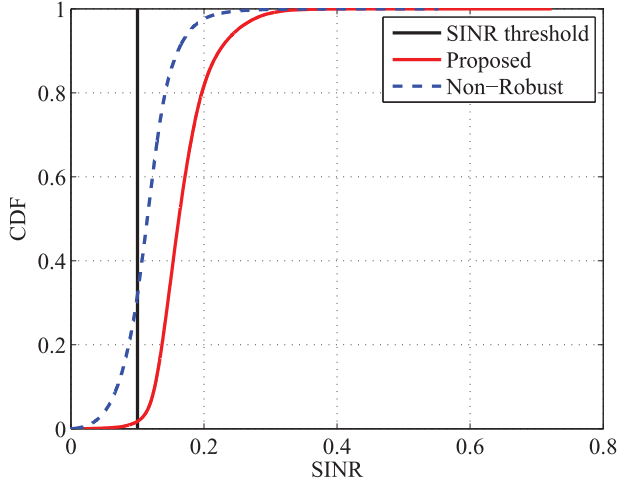
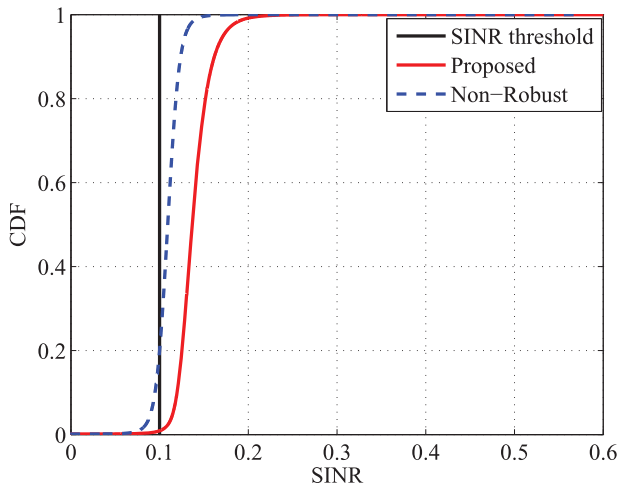Fig. 11. SINR cumulative distribution function (S1).

Fig. 12. SINR cumulative distribution function (S2).

the greedy scheme is decreasing in r, with lower performance gain relative to VQOC.

Finally, the performance of the worst-case SINR design [cf. (4)–(6)] is demonstrated in Figs. 11 and 12. The black solid line indicates the SINR threshold $\gamma_k = 0.1$, $\forall k$. The non-robust scheme simply treats the estimated channel $\hat{\mathbf{h}}_k^t$ as the actual one, and plugs it into the SINR constraint $\text{SINR}_k(\{\mathbf{w}_k^t\}) \geq \gamma_k$. This constraint can be transformed into a linear matrix inequality $\hat{\mathbf{h}}_k^{tH}\mathbf{Y}_k^t\hat{\mathbf{h}}_k^t - \sigma_k^2 \geq 0$, which is a relaxed version of our proposed counterpart in (12). For both the robust and non-robust approaches, each transmit beamformer $\mathbf{w}_k^t$ is obtained as the principal eigenvector associated with the largest eigenvalue of the optimal $\mathbf{X}_k^t$. The cumulative density function of the actual SINR is then available by evaluating (2) with 1, 000 i.i.d. channel realizations. In Fig. 11, there are 30% of the realizations violating the SINR constraint for the non-robust scheme, while only about 1.5% for the proposed approach. Similarly, for (S2) in Fig. 12, the non-robust scheme violates the SINR constraint 20% of the time with SINR violation, while only 0.9% for our novel scheme. Note that the SINR constraint violation of the proposed approach are due to the possibly inexact SDP relaxation.

VI. Conclusions

In this paper, real-time energy management and robust transmit beamforming designs were developed for smart-grid powered CoMP transmissions. Leveraging the distributed storage units, base stations are able to trade shortage or surplus energy with the main grid to maintain the operations. Taking into account the uncertainties of both channel estimation and harvested renewables, a stochastic optimization problem was formulated to minimize the expected transaction cost while satisfying the worst-case QoS requirements. Clearly, batch schemes cannot be devised due to the infinite horizon. Inspired by Lyapunov optimization techniques, a virtual-queue based online algorithm was thus developed to obtain feasible decisions 'on-the-fly' by relaxing the time-coupling constraints arising due to the storage dynamics. Interestingly, the novel method was proved asymptotically optimal even without knowing the probability density function of the underlying stochastic processes. Extensive numerical tests justify the effectiveness and merits of the proposed approach for both i.i.d. and non-i.i.d. scenarios.

The present framework opens new directions for green wireless communications that aim at utilizing effectively energy sources. Interesting future works include e.g., the incorporation of DC/AC power flows, contingency constraints, battery-health conscious dynamic scheduling, as well as various types of storage units. Moreover, probability SINR constraints and different uncertainty sets are worth investigating.

References

[1] R. Irmer *et al.*, "Coordinated multipoint: Concepts, performance, and field trial results," *IEEE Commun. Mag.*, vol. 49, no. 2, pp. 102–111, Feb. 2011.

[2] H. Dahrouj and W. Yu, "Coordinated beamforming for the multicell multi-antenna wireless system," *IEEE Trans. Wireless Commun.*, vol. 9, no. 5, pp. 1748–1759, May 2010.

[3] J. Zhang, R. Chen, J. Andrews, A. Ghosh, and R. W. Heath, "Networked MIMO with clustered linear precoding," *IEEE Trans. Wireless Commun.*, vol. 8, no. 4, pp. 1910–1921, Apr. 2009.

[4] C. Ng and H. Huang, "Linear precoding in cooperative MIMO cellular networks with limited coordination clusters," *IEEE J. Sel. Areas Commun.*, vol. 28, no. 9, pp. 1446–1454, Dec. 2010.

[5] 3TIER. (2006). *Western Wind Resources Dataset* [Online]. Available: http://wind.nrel.gov/Web_nrel/

[6] CAISO. (2015). *Daily Renewable Output Data* [Online]. Available: http://www.caiso.com/green/renewableswatch.html

[7] E. Oh, B. Krishnamachari, X. Liu, and Z. Niu, "Toward dynamic energy-efficient operation of cellular network infrastructure," *IEEE Commun. Mag.*, vol. 49, no. 6, pp. 56–61, Jun. 2011.

[8] A. Tolli, H. Pennanen, and P. Komulainen, "Decentralized minimum power multi-cell beamforming with limited backhaul signaling," *IEEE Trans. Wireless Commun.*, vol. 10, no. 2, pp. 570–580, Feb. 2011.

[9] Y. Shi, J. Zhang, and K. Letaief, "Group sparse beamforming for green cloud-RAN," *IEEE Trans. Wireless Commun.*, vol. 13, no. 5, pp. 2809–2823, May 2014.

[10] Y. Zhang, N. Gatsis, and G. B. Giannakis, "Robust energy management for microgrids with high-penetration renewables," *IEEE Trans. Sustain. Energy*, vol. 4, no. 4, pp. 944–953, Oct. 2013.

[11] X. Liu and W. Xu, "Economic load dispatch constrained by wind power availability: A here-and-now approach," *IEEE Trans. Sustain. Energy*, vol. 1, no. 1, pp. 2–9, Apr. 2010.

[12] X. Guan, Z. Xu, and Q. Jia, "Energy-efficient buildings facilitated by microgrid," *IEEE Trans. Smart Grid*, vol. 1, no. 3, pp. 243–252, Dec. 2010.

[13] G. B. Giannakis, V. Kekatos, N. Gatsis, S. Kim, H. Zhu, and B. Wollenberg, "Monitoring and optimization for power grids: A signal processing perspective," *IEEE Signal Process. Mag.*, vol. 30, no. 5, pp. 107–128, Sep. 2013.

[14] S. Bu, F. Yu, Y. Cai, and X. Liu, "When the smart grid meets energy-efficient communications: Green wireless cellular networks powered by the smart grid," *IEEE Trans. Wireless Commun.*, vol. 11, no. 8, pp. 3014–3024, Aug. 2012.

[15] J. Xu, Y. Guo, and R. Zhang, "CoMP meets energy harvesting: A new communication and energy cooperation paradigm," in *Proc. Globecom*, Atlanta, GA, USA, Dec. 2013, pp. 2508–2513.

[16] J. Xu and R. Zhang, "Cooperative energy trading in CoMP systems powered by smart grids," *IEEE Trans. Veh. Technol.*, vol. 65, no. 5, May 2016.

[17] D. Niyato, X. Lu, and P. Wang, "Adaptive power management for wireless base stations in a smart grid environment," *IEEE Wireless Commun.*, vol. 19, no. 6, pp. 44–51, Dec. 2012.

[18] X. Wang, Y. Zhang, G. B. Giannakis, and S. Hu, "Robust smart-grid powered cooperative multipoint systems," *IEEE Trans. Wireless Commun.*, vol. 14, no. 11, pp. 6188–6199, Nov. 2015.

[19] R. Urgaonkar, B. Urgaonkar, M. Neely, and A. Sivasubramaniam, "Optimal power cost management using stored energy in data centers," in *Proc. ACM SIGMETRICS*, San Jose, CA, USA, Jun. 2011, pp. 221–232.

[20] S. Lakshminaryana, H. V. Poor, and T. Quek, "Cooperation and storage trade-offs in power grids with renewable energy resources," *IEEE J. Sel. Areas Commun.*, vol. 32, no. 7, pp. 1–12, Jul. 2014.

[21] L. Georgiadis, M. Neely, and L. Tassiulas, "Resource allocation and cross-layer control in wireless networks," *Found. Trends Netw.*, vol. 1, pp. 1–144, 2006.

[22] N. Vucic and H. Boche, "Robust QoS-constrained optimization of downlink multiuser MISO systems," *IEEE Trans. Signal Process.*, vol. 57, no. 2, pp. 714–725, Jun. 2009.

[23] F. Genoese, M. Genoese, and M. Wietschel, "Occurrence of negative prices on the German spot market for electricity and their influence on balancing power markets," in *Proc. 7th Int. Conf. Eur. Energy Market*, Madrid, Spain, Jun. 2010, pp. 1–6.

[24] I. Polik and T. Terlaky, "A survey of the S-lemma," *SIAM Rev.*, vol. 49, no. 3, pp. 371–418, 2007.

[25] D. P. Bertsekas, *Convex Optimization Theory*. Belmont, MA, USA: Athena Scientific, 2009.

[26] A. Stolyar, "Maximizing queueing network utility subject to stability: Greedy primal-dual algorithm," *Queueing Syst.*, vol. 50, pp. 401–457, 2005.

[27] X. Wang, G. B. Giannakis, and A. Marques, "A unified approach to QoS-guaranteed scheduling for channel-adaptive wireless networks," *Proc. IEEE*, vol. 95, no. 12, pp. 2410–2431, Dec. 2007.

[28] A. Eryilmaz and R. Srikant, "Fair resource allocation in wireless networks using queue-length-based scheduling and congestion control," *IEEE/ACM Trans. Netw.*, vol. 15, no. 6, pp. 1333–1344, Dec. 2007.

[29] N. Gatsis, A. Ribeiro, and G. B. Giannakis, "A class of convergent algorithms for resource allocation in wireless fading networks," *IEEE Trans. Wireless Commun.*, vol. 9, no. 5, pp. 1808–1823, May 2010.

[30] M. Grant, S. Boyd, and Y. Ye. (2012, Sep.). *CVX: Matlab Software for Disciplined Convex Programming, version 2.1* [Online]. Available: http://cvxr.com/cvx

[31] E. Song, Q. Shi, M. Sanjabi, R. Sun, and Z.-Q. Luo, "Robust SINR-constrained MISO downlink beamforming: When is semidefinite programming relaxation tight?" *EURASIP J. Wireless Commun. Netw.*, vol. 2012, no. 243, pp. 1–11, Aug. 2012, doi: 10.1186/1687-1499-2012-243

[32] P. Tseng, "Further results on approximating nonconvex quadratic optimization by semidefinite programming relaxation," *SIAM J. Optim.*, vol. 14, no. 1, pp. 268–283, Jul. 2003.

[33] K. C. Toh, M. J. Todd, and R. H. Tutuncu, "SDPT3—A Matlab software package for semidefinite programming," *Optim. Methods Softw.*, vol. 11, pp. 545–581, 2009.

[34] Y. Zhang, N. Gatsis, and G. B. Giannakis, "Risk-constrained energy management with multiple wind farms," in *Proc. 4th IEEE-PES Innov. Smart Grid Technol.*, Washington, DC, USA, Feb. 2013, pp. 1–6.

[35] National Grid. (2015, Jan.). *Hourly Electric Supply Charges in New York* [Online]. Available: https://www.nationalgridus.com/

[36] PJM. (2015, Jan.). *Pennsylvania-New Jersey-Maryland Interconnection (PJM) Hourly Real-Time Wind Generation* [Online]. Available: http://www.pjm.com/markets-and-operations/ops-analysis.aspx

[37] Samsung SDI. (2015). *Samsung Energy Storage System* [Online]. Available: http://www.samsungsdi.com/ess/overview

[38] Y. Yao, L. Huang, A. Sharma, L. Golubchik, and M. Neely, "Data centers power reduction: A two time scale approach for delay tolerant workloads," in *Proc. INFOCOM*, Orlando, FL, USA, Mar. 2012, pp. 1431–1439.

Xin Wang (SM'09) received the B.Sc. and M.Sc. degrees from Fudan University, Shanghai, China, in 1997 and 2000, respectively, and the Ph.D. degree from Auburn University, Auburn, AL, USA, in 2004, all in electrical engineering. From September 2004 to August 2006, he was a Postdoctoral Research Associate with the Department of Electrical and Computer Engineering, University of Minnesota, Minneapolis, MN, USA. In August 2006, he joined the Department of Computer and Electrical Engineering and Computer Science, Florida Atlantic University, Boca Raton, FL, USA, as an Assistant Professor and, in August 2010, was promoted and became an Associate Professor. He is currently a Professor with the Department of Communication Science and Engineering, Fudan University. His research interests include stochastic network optimization, energy-efficient communications, cross-layer design, and signal processing for communications. He served as an Associate Editor for the IEEE SIGNAL PROCESSING LETTERS. He currently serves as an Associate Editor for the IEEE TRANSACTIONS ON SIGNAL PROCESSING and as an Editor for the IEEE TRANSACTIONS ON VEHICULAR TECHNOLOGY.

Yu Zhang (S'11) received the B.Eng. and M.Sc. degrees (both with highest Hons.) from Wuhan University of Technology, Wuhan, China, and from Shanghai Jiao Tong University, Shanghai, China, in 2006 and 2010, respectively, and the Ph.D. degree from the University of Minnesota, Minneapolis, MN, USA, in 2015, all in electrical engineering. He is currently a Postdoctoral Associate with the Department of Electrical and Computer Engineering, University of Minnesota. His research interests include smart power grids, optimization theory, machine learning, distributed energy management with renewables, and energy data analytics. He was the recipient of the Huawei Scholarship and the Infineon Scholarship from the Shanghai Jiao Tong University (2009), the ECE Department Fellowship from the University of Minnesota (2010), and the Student Travel Awards from the SIAM and the IEEE Signal Processing Society (2014).
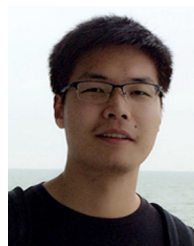
Tianyi Chen (S'15) received the B.Eng. degree (with highest Hons.) in communication science and engineering from Fudan University, Shanghai, China, in 2014. He is currently pursuing the Ph.D. degree in ECE at the University of Minnesota, Minneapolis, MN, USA. Since August 2014, he has been with SPiNCOM. His research interests include network optimization with applications to green communications, and sustainable data centers. He received a National Scholarship from China in 2013, and the UMN ECE Department Fellowship in 2014.

Georgios B. Giannakis (F'97) received the Diploma degree in electrical engineering from the National Technical University of Athens, Athens, Greece, in 1981, the M.Sc. degree in electrical engineering, the M.Sc. degree in mathematics, and the Ph.D. degree in electrical engineering from the University of Southern California (USC), Los Angeles, CA, USA, in 1983, 1986, and 1986, respectively. Since 1999, he has been a Professor with the University of Minnesota, Minneapolis, MN, USA, where he now holds an ADC Chair in Wireless Telecommunications, ECE Department, and serves as the Director of the Digital Technology Center. He has authored more than 385 journal papers, 650 conference papers, 22 book chapters, 2 edited books and 2 research monographs (h-index 115). His research interests include communications, networking and statistical signal processing, Big Data, wireless cognitive radios, and network science with applications to social, brain, and power networks with renewables. He is the Co-Inventor of 25 patents issued. He is a Fellow of EURASIP, and has served the IEEE in a number of posts, including that of a Distinguished Lecturer for the IEEE-SP Society. He was the corecipient of the 8 Best Paper Awards from the IEEE Signal Processing (SP) and Communications Societies, including the G. Marconi Prize Paper Award in Wireless Communications. He was also the recipient of the Technical Achievement Awards from the SP Society (2000), from EURASIP (2005), a Young Faculty Teaching Award and the G. W. Taylor Award for Distinguished Research from the University of Minnesota, and the IEEE Fourier Technical Field Award (2015).